https://doi.org/10.5194/egusphere-2026-862
Preprint. Discussion started: 27 February 2026

Brief communication: First-year MRR observations at Great Wall Station, Antarctic Peninsula region

Jiayi Sun[1], Junmei Lv[1], Haoran Li[1*], Wenqian Zhang[1], Biao Tian[1], Minghu Ding[1,2*]

[1]State Key Laboratory of Severe Weather Meteorological Science and Technology, Chinese Academy of Meteorological Sciences, Beijing, China.
[2]Key Laboratory of Polar Atmosphere−Ocean−Ice System for Weather and Climate, Ministry of Education, Shanghai, China.

Correspondence to: Haoran Li (lihr@cma.gov.cn) and Minghu Ding(dingmh@cma.gov.cn)

Abstract. We report the first-year (March 2024–November 2025) of observations of a Micro Rain Radar (MRR) deployed at Great Wall Station in the Antarctic Peninsula. We imposed quality control to raw MRR data and identified a surface precipitation (snowfall) occurrence of 0.32 (0.23). The median radar reflectivity of snowfall is approximately 9 dBZ, exhibiting minimal variation with height as caused by frequent shallow snowfall. Blowing snow can significantly increase (decrease) the snow occurrence (median radar reflectivity) to as high as 0.7 km. We further developed a localized Z_e (equivalent radar reflectivity) – S (snowfall rate) parameterization, and identified a systematic underestimation of cumulative snowfall profiles in ERA5 products.

1 Introduction

The Antarctic Ice Sheet contains a substantial fraction of Earth's land ice; consequently, perturbations in its mass budget have the potential to exert a measurable influence on global mean sea level(DeConto and Pollard, 2016; Morlighem et al., 2020). A key metric for characterizing atmosphere–ice exchange is the surface mass balance (SMB). Across most of Antarctica, the gain term of SMB is dominated by solid precipitation—predominantly snowfall—thereby providing the primary pathway for net surface snow accumulation (van Wessem et al., 2018). Hence, precipitation represents a cornerstone variable for diagnosing present-day Antarctic SMB and constraining its future evolution. Yet, direct precipitation observations over Antarctica remain severely limited.

Due to the harsh natural conditions and low temperatures in Antarctica, maintaining long-term precipitation observations in this region is challenging(Ding et al., 2022b). Satellite products and numerical models currently underpin much of the research on Antarctic precipitation. Spaceborne radars

https://doi.org/10.5194/egusphere-2026-862
Preprint. Discussion started: 27 February 2026

have made continent-scale detection feasible; however, their utility for diagnosing precipitation evolution through the atmospheric column—and, in particular, near-surface depletion processes such as sublimation—is substantially curtailed by the combination of coarse temporal sampling, restricted spatial coverage (CloudSat typically limited to north of ~82° S), and a pronounced low-level observational gap associated with the radar blind zone (Alexander et al., 2023; Grazioli et al., 2017a). Compounding these limitations, the paucity of ground-based precipitation observations across Antarctica precludes rigorous, process-oriented validation of model and reanalysis products; moreover, many model parameterizations—having been developed primarily for mid-latitude regimes—are not tailored to the Antarctic environment, which contributes to systematic deviations from available local observations (Agosta et al., 2015)

Ground-based remote sensing can provide high-temporal-resolution profile measurements, making it possible to observe precipitation through the atmospheric column—from formation aloft to the near-surface layers—and, at the same time, to benchmark numerical model performance against independent observations. In particular, vertical profiles from Micro Rain Radars (MRRs) have been used to develop site-specific reflectivity–snowfall-rate ($Z_e = aS^b$) relationships over East Antarctica (some of the red circles in Fig. 1a). Souverijns et al. (2017) derived such a relation by combining observations from the first Antarctic MRR with measurements from a precipitation imaging instrument (PIP) deployed at Princess Elisabeth Station. Scarchilli et al. (2020) similarly estimated an MZS Z_e–S relation using an MRR installed at the Italian Mario Zucchelli Station together with co-located snow-gauge observations. At Dumont d'Urville (DDU), Grazioli et al. (2017b) presented the first results from precipitation monitoring that integrated an MRR with gauge measurements, and Grazioli, Madeleine, et al. (2017a) further showed—through comparison with model outputs—that katabatic winds can strongly enhance low-level snowfall sublimation. During the YOPP-SH special observing campaign at DDU, Roussel et al. (2023) combined gauge and MRR observations to assess the ability of several atmospheric models and meteorological reanalyses to represent snowfall occurrence. More recently, Wiener et al. (2024) compiled and analyzed a seven-year MRR profiling record at DDU and used it to evaluate model performance. An MRR has also been deployed at Davis; although no site-specific Z_e–S relationship has been reported to date, Alexander et al. (2023) used a K-band MRR and a W-band cloud radar to

https://doi.org/10.5194/egusphere-2026-862
Preprint. Discussion started: 27 February 2026

characterize the vertical structure and microphysics of coastal Antarctic snowfall, and showed that Föhn-driven boundary-layer sublimation can remove about 50% of snowfall mass within CloudSat's near-surface blind zone.

Rising temperatures associated with ongoing climate change place austral-summer conditions in the coastal Antarctic Peninsula frequently near the 0 °C threshold, making the precipitation phase (rain versus snow) particularly sensitive to thermodynamic fluctuations and circulation perturbations. (Ding et al., 2020). However, continuous observations of precipitation processes in this region have yet to be reported, leaving a gap in the evaluation of model simulations of precipitation over the area. In this study, we address this gap with the first-year MRR observations collected at Great Wall Station.

2 Data and methods

2.1 Great Wall Station

Figure 1a shows the location of the observation site used in this study, China's Great Wall Station (62°13′ S, 58°58′ W; 10 m a.s.l.). The station is situated on the coastal margin of the Fildes Peninsula on the western part of King George Island, in the South Shetland Islands, northwest of the Antarctic Peninsula. The construction and operation of the station's surface meteorological instrumentation and observing procedures follow the standards of the World Meteorological Organization (WMO) and the China Meteorological Administration (CMA) (Ding et al., 2020), Great Wall Station was established in 1985, and continuous 24 h automatic observations have been conducted since 2002. Figures 1b$_1$–b$_3$ present, respectively, the daily-mean wet-bulb temperature, daily-mean relative humidity, and daily-mean wind speed recorded by the automatic weather station from 10 March 2024 to 30 November 2025; the wet-bulb temperature was calculated from the measured air temperature in combination with surface pressure and relative humidity.

https://doi.org/10.5194/egusphere-2026-862
Preprint. Discussion started: 27 February 2026

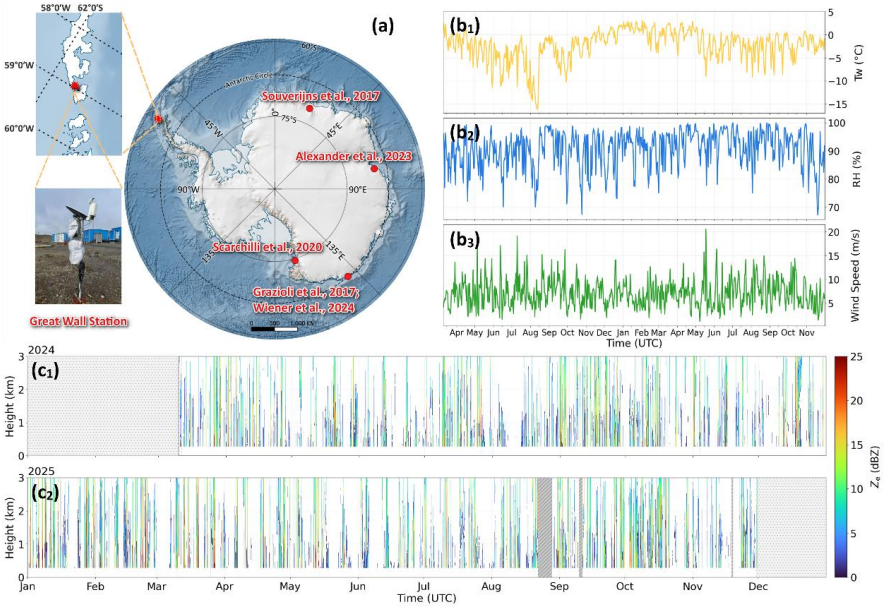

Figure 1 (a) Location of Great Wall Station and the deployed Micro Rain Radar (MRR), together with the automatic weather station (AWS). (b_1) Daily-mean wet-bulb temperature T_w (yellow solid line) (b_2) Daily-mean relative humidity (blue solid line). (b_3) Daily-mean wind speed (green solid line). (c_1)–(c_2) Equivalent radar reflectivity (Z_e) for 2024 and 2025, respectively. Grey hatched areas indicate periods of missing data. In (a), established MRR sites are marked with red dots, and scholars who used MRR data from the corresponding sites are annotated.

2.2 Micro Rain Radar

Deployed at China's Great Wall Station in early 2024, the Micro Rain Radar (MRR; K-band, 24 GHz) is a vertically pointing frequency-modulated continuous-wave (FM-CW) Doppler system (see the lower-left panel of Fig. 1). Panels c_1 and c_2 of Figure 1 summarize the timing of precipitation events over the full observation period together with the associated intensity variability. With the exception of two short data gaps caused by an SD-card malfunction (23–27 August 2025 and 10 September 2025), the record is essentially continuous, yielding 625 days of effective measurements.

All MRR spectra were processed using a Doppler-spectra-based processing framework following Maahn and Kollias (2012) which is designed to enhance performance under low signal-to-noise conditions typical of snowfall. We also identified and removed stationary noise signals by temporally averaging

https://doi.org/10.5194/egusphere-2026-862
Preprint. Discussion started: 27 February 2026

spectral observations as used by Ding et al. (2022a). The procedure applies robust noise suppression and a dynamic dealiasing strategy, thereby improving the retrieval of weak spectral signatures (including subtle vertical-motion signals) and increasing the detectability of light precipitation. For the snowfall statistics, time steps with no valid return at the lowest usable range gate (~300 m above ground level) were treated as snow-free. In addition, profiles exhibiting a bright band associated with the 0 °C melting layer aloft (Li et al., 2020; Li and Moisseev, 2020) were excluded from the snowfall classification and were not counted as snowfall.

2.3 ERA5 products

The ERA5 atmospheric reanalysis produced by the European Centre for Medium-Range Weather Forecasts is used in this study. ERA5 is generated with the IFS global forecasting system (CY41R2) coupled with a four-dimensional data assimilation framework, providing a wide range of atmosphere–land–ocean variables on an approximately 30 km horizontal grid and a 137-level vertical discretization; although ERA5 records extend to years earlier than 1979, 1979 is commonly regarded as the earliest reliable year for Southern Hemisphere analyses, and ERA5 is therefore widely used as the successor to ERA-Interim. Hourly ERA5 data from March 2024 to November 2025 are analysed. To ensure consistency with radar-derived vertical precipitation profiles, archived surface precipitation is not used directly. Instead, following the approach described in the Supplement (Sect. S3) of Roussel et al. (2023), model-level solid precipitation flux diagnostics defined at the midpoints of the IFS vertical layers are employed to reconstruct height-resolved snowfall amounts, thereby producing snowfall profile products that are directly comparable to the observed vertical structure.

https://doi.org/10.5194/egusphere-2026-862
Preprint. Discussion started: 27 February 2026

3 Results

3.1 Precipitation occurrence

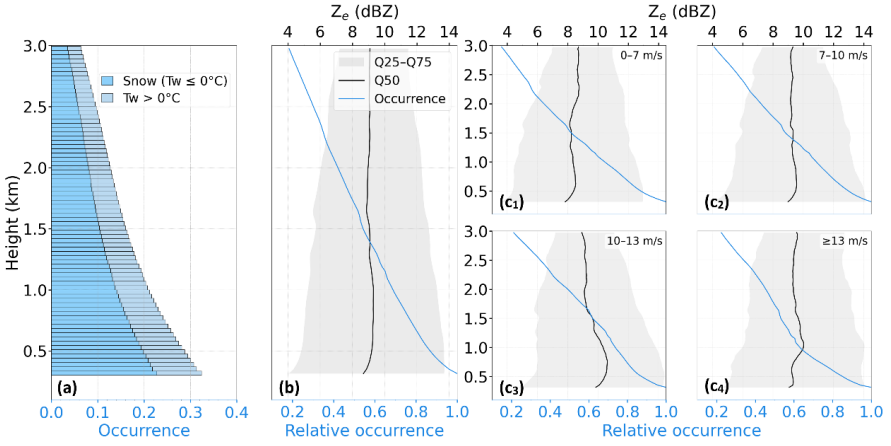

Figure 2(a) Precipitation occurrence probability at Great Wall Station as a function of height (light blue: snowfall; dark blue: wet snow and rain). (b) Vertical profiles of equivalent radar reflectivity (Z_e) for snowfall. (c_1)–(c_4) Snowfall Z_e statistics stratified by wind-speed regimes: 0–7 m s^{-1} (c_1), 7–10 m s^{-1} (c_2), 10–13 m s^{-1} (c_3), and ≥13 m s^{-1} (c_4). For each regime, the median Z_e is shown by the black solid line, the interquartile range (25th, 75th percentiles) by the light-grey shading, and the height-dependent relative frequency of snowfall occurrence by the blue solid line.

In this study, the observed reflectivity (Z_e) is used to quantify the height-dependent occurrence frequency of precipitation at Great Wall Station (Fig. 2a). The vertical binning follows the native range resolution of the MRR (35 m). Figure 2a clearly shows a monotonic decrease in precipitation occurrence with height, with total precipitation occurrence ranging from 6.4% to 32.4% across the sampled column. At 0.3 km a.g.l., snowfall occurs 22.8% of the time, whereas wet snow and rain account for 9.6%; at 3.0 km a.g.l. , the corresponding frequencies decrease to 3.5% for snowfall and 2.9% for wet snow and rain. Overall, the lower layers are dominated by snowfall. With increasing height, precipitation occurrence decreases, and the reduction is more pronounced for snowfall—the dominant phase near the surface—so that the difference between snowfall and wet snow/rain progressively narrows. This implies that snowfall is more frequent than rainfall near the surface, whereas at higher levels snowfall and rainfall occur with comparable frequency.

https://doi.org/10.5194/egusphere-2026-862
Preprint. Discussion started: 27 February 2026

To further characterize the snowfall regime, snowfall-only Z_e profiles are examined (Fig. 2b). The median reflectivity during snowfall exhibits only weak vertical variability, remaining close to ~9 dBZ throughout most of the profile. A modest enhancement around ~1.25 km is consistent with microphysical growth processes, including aggregation and riming, as well as vapor-deposition growth and sublimation effects (Planat et al., 2021). Below ~0.7 km, a slight decrease is observed; however, unlike the MRR-based statistics reported at DDU (Wiener et al., 2024), the reduction in Z_e beneath 0.7 km is not pronounced at Great Wall Station. Because strong low-level reflectivity decreases at DDU have been linked to katabatic-flow-driven sublimation of falling snow(Grazioli et al., 2017a) , the comparatively weak near-surface decrease at Great Wall Station suggests a limited katabatic influence in the Antarctic Peninsula coastal setting. This interpretation is physically consistent with the katabatic-wind mechanism—dry, downslope flow originating from the interior plateau—given that Great Wall Station is not located within a prominent katabatic outflow corridor. Finally, a comparison of the 25th and 75th percentile envelopes with those reported for DDU indicates that Great Wall Station frequently experiences low-topped, long-lasting, and weak snowfall events. The prevalence of these low-intensity cases increases the contribution of weak low-level returns, leading to a downward tendency in the 25th-percentile Z_e profile toward the surface, while leaving the median profile relatively invariant with height.

3.2 Signatures of blowing snow

Blowing snow is a ubiquitous phenomenon in Antarctic continent. Using a multi-instrument (MI) algorithm at McMurdo Station in West Antarctica, Loeb and Kennedy (2023) reported a mean blowing-snow layer thickness of approximately 168.2 m; however, the wind-speed dependence of snowfall reflectivity profiles was not examined in detail. Motivated by this gap, snowfall Z_e profiles at Great Wall Station were further stratified by wind speed measured by the co-located automatic weather station. Previous studies have noted that blowing-snow effects become non-negligible for wind speeds exceeding 7 m s^{-1} when deriving Z_e–S relationships(Scarchilli et al., 2020; Wiener et al., 2024). Accordingly, wind speed was binned into four regimes: 0–7 m s^{-1} (Fig. 2c_1), 7–10 m s^{-1} (Fig. 2c_2), 10–13 m s^{-1} (Fig. 2c_3), and ≥13 m s^{-1} (Fig. 2c_4). Under the two lower-wind regimes (Figs. 2c_1–c_2), the snowfall Z_e profiles

https://doi.org/10.5194/egusphere-2026-862
Preprint. Discussion started: 27 February 2026

closely resemble the aggregate snowfall statistics, exhibiting only weak height dependence. By contrast, for wind speeds of 10–13 m s^{-1} (Fig. 2c_3), a marked enhancement of low-level reflectivity emerges. When wind speed exceeds 13 m s^{-1} (Fig. 2c_4), a pronounced reduction in Z_e occurs below 1 km, accompanied by an abrupt decrease in the relative frequency of snowfall occurrence at 1 km—from about 70% in Figure 2c_3 to roughly 60%—and, toward lower altitudes, a noticeably steeper vertical gradient in the occurrence profile. This pattern is consistent with strong-wind impacts on the near-surface snow field: enhanced sublimation and turbulent mixing can reduce the abundance of larger falling snowflakes, while resuspension of previously deposited, smaller particles injects numerous low-reflectivity targets into the lowest layers, thereby shifting the distribution of radar returns toward weaker Z_e. Collectively, these results indicate that the Great Wall Station MRR is able to detect and characterize the influence of high wind speeds on the vertical structure of snowfall.

https://doi.org/10.5194/egusphere-2026-862
Preprint. Discussion started: 27 February 2026

3.3 Cumulative snowfall profiles and model evaluation

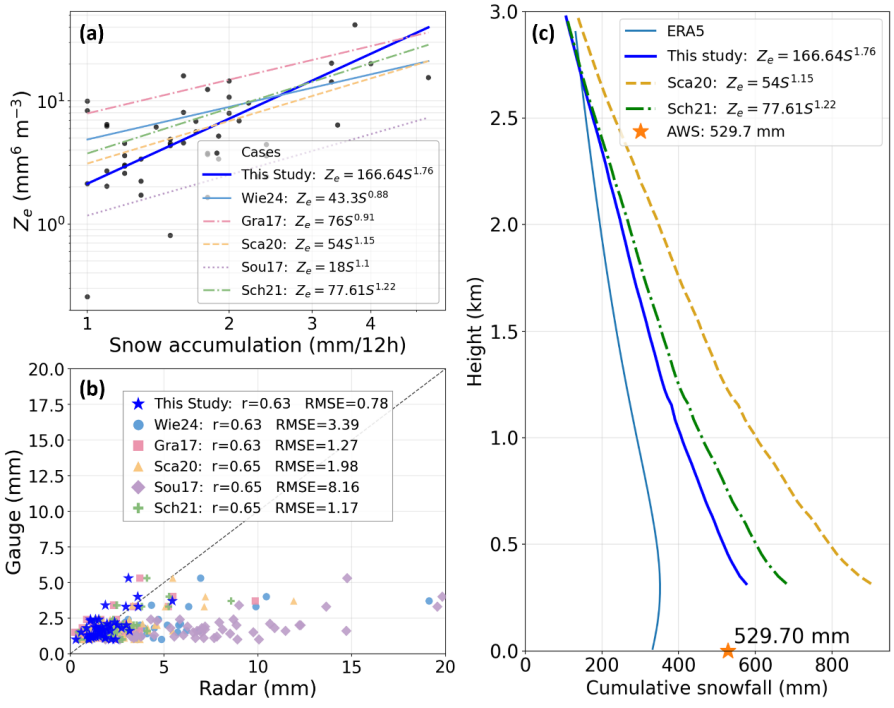

Figure 3 (a) Scatterplot of MRR equivalent reflectivity (linear units) versus 12 h snowfall accumulation from the automatic weather station (black dots), together with the Z_e–S relationship derived using DE regression (solid blue line). Also shown are published Z_e–S relations from Wiener et al. (2024) **(light-blue solid), Grazioli et al.** (2017b) **(red dashed), Scarchilli et al.** (2020) **(yellow dashed), Souverijns et al**. (2017) **(purple dashed) and Schoger et al.** (2021) **(green dashed). (b) Comparison between 12 h snowfall accumulation estimated from MRR reflectivity using the same Z_e–S relations as in (a) and the time-scheduled precipitation amounts recorded by the automatic weather station (scatterplot). (c) Cumulative snowfall profiles from ERA5 and from the MRR-based retrieval using the locally fitted relation (solid blue), together with profiles computed using the relations of Scarchilli et al.** (2020) **(yellow dashed) and Schoger et al.** (2021) **(green dashed).**

In Figure 3a, a site-specific $Z_e = aS^b$relationship for the Great Wall Station MRR is derived by pairing radar equivalent reflectivity Z_e (mm^6m^{-3}) with 12 h snowfall accumulation S (mm per 12 h) measured by the automatic weather station, and estimating the parameters $a$and $b$using a differential-evolution (DE) optimization algorithm. This approach is widely adopted for retrieving snowfall rate from radar reflectivity and has been applied in numerous Antarctic studies (Grazioli et al., 2017b; Scarchilli et

https://doi.org/10.5194/egusphere-2026-862
Preprint. Discussion started: 27 February 2026

al., 2020; Schoger et al., 2021; Souverijns et al., 2017; Wiener et al., 2024). For the fit, Z_e at the lowest usable radar range gate (approximately 300 m a.g.l.) is used and converted to linear units (mm^6m^{-3}). However, not all observations are suitable for constructing a robust Z_e–S relation. In particular, strong horizontal winds can resuspend previously deposited snow, leading to biased gauge accumulations and, consequently, biased regression. Therefore, the cases used in Figure 3a (black circles) are restricted to snowfall periods with wind speeds of 0–7 m s^{-1}. In addition, to minimize contamination by liquid precipitation, the 12 h accumulation window is required to contain no time steps with wet-bulb temperature $T_w > 0$°C. Applying these filters yields the subset shown by the black points in Figure 3a. The resulting best-fit parameters are $a = 166.64$ and $b = 1.76$, i.e., $Z_e = 166.64\,S^{1.76}$, plotted as the solid blue line. For reference, several published Z_e–S relations are also overlaid in Figure 3a using distinct colors. To assess fitting performance and potential bias, Figure 3b compares 12 h snowfall accumulations estimated from MRR reflectivity using each Z_e–S relation against the corresponding 12 h accumulations recorded by the automatic weather station; the color coding matches that in Figure 3a. Although the locally fitted relation yields a correlation coefficient $R = 0.63$, it achieves the smallest root-mean-square error (RMSE = 0.78) and the lowest bias among the tested relations. Among the published relations, those of Scarchilli et al.(2020), $Z_e = 54\,S^{1.15}$(yellow), and Schoger et al.(2021) $Z_e = 77.61\,S^{1.22}$ (green), perform comparatively well, both producing $R = 0.65$ with RMSE values of 1.98 and 1.17, respectively.

Building on the fitted relationship $Z_e = 166.64\,S^{1.76}$, together with the power-law relations proposed by Scarchilli et al.(2020), and Schoger et al. (2021), cumulative snowfall profiles at Great Wall Station were computed for 10 March 2024 to 30 November 2025 (Fig. 3c) and compared with the cumulative snowfall profile derived from ERA5 (Fig. 3c). Figure 3c indicates that ERA5 substantially underestimates cumulative snowfall relative to the MRR-based estimates: the ERA5 maximum occurs near 300 m a.g.l. and reaches only ~340 mm, which is not only smaller than the MRR-derived accumulation at the same height but also lower than the surface accumulation recorded by the automatic weather station (~530 mm). In contrast, the MRR-derived accumulation at the lowest usable gate (~300 m a.g.l.) exceeds the gauge total for all tested Z_e–S relations; using the locally fitted relation yields an accumulation of ~560 mm at 300 m. This result highlights the value of profiling radar observations for

https://doi.org/10.5194/egusphere-2026-862
Preprint. Discussion started: 27 February 2026

snowfall quantification, as the vertically resolved radar retrieval provides a more robust estimate of snowfall accumulation than surface gauge records that are susceptible to wind-related biases. ERA5 reproduces the general increase in cumulative snowfall from the top of the profile down to approximately 300 m, consistent with the MRR-derived profiles, but the increase is weaker, i.e., the vertical gradient is insufficiently steep. Moreover, ERA5 exhibits a decrease in cumulative snowfall below ~300 m, consistent with strong near-surface depletion associated with sublimation, whereas the MRR-based profiles do not show a comparable near-surface reduction, suggesting a limited imprint of katabatic-flow-driven sublimation at Great Wall Station. This contrasts with previous work at Dumont d'Urville (DDU), where ERA5 cumulative snowfall profiles typically peak at ~0.8–1.0 km before decreasing toward the surface(Grazioli et al., 2017a; Roussel et al., 2023; Wiener et al., 2024). At Great Wall Station, by comparison, the ERA5 maximum is attained much lower—near ~300 m—before any decrease is simulated. Taken together with the snowfall reflectivity statistics discussed in Sect. 2.3.1, these results support the conclusion that katabatic influence on near-surface snowfall at Great Wall Station is comparatively weak.

4 Discussion and conclusion

This study analyzes the first Micro Rain Radar (MRR) precipitation profiling dataset collected at Great Wall Station in the Antarctic Peninsula sector during March 2024–November 2025. The resulting observations provide a useful case study demonstrating the practical value of ground-based precipitation monitoring at Great Wall Station and offering an observational basis for characterizing precipitation features in the surrounding Antarctic Peninsula region.

Based on a statistical analysis of the MRR precipitation profiles and an ERA5 evaluation enabled by a locally fitted Z_e–S relationship derived for Great Wall Station, the main findings of this report are as follows:

1. In terms of precipitation occurrence, precipitation is detected in the lower levels at Great Wall Station about 32.4% of the time, with pure snowfall accounting for 22.8%, indicating an overall snowfall-dominated regime. Total precipitation occurrence decreases with height: snowfall dominates at low levels, whereas at higher altitudes the occurrence frequencies of snowfall and wet snow/rain become comparable.

https://doi.org/10.5194/egusphere-2026-862
Preprint. Discussion started: 27 February 2026

2. Statistics of equivalent reflectivity during snowfall further show that the median snowfall reflectivity exhibits no pronounced vertical variation and remains close to ~9 dBZ. Compared with Dumont d'Urville (DDU), the near-surface imprint of katabatic-flow-driven effects is not as strong, and Great Wall Station features a larger fraction of low-topped, persistent, and weak snowfall events.

3. The MRR reflectivity observations appear to be only weakly affected for wind speeds below 10 m s^{-1}; when wind speed is 10–13 m s^{-1}, the low-level reflectivity increases markedly. For wind speeds ≥13 m s^{-1}, reflectivity within 0.5–1 km decreases substantially, consistent with the resuspension of surface snow, while the relative frequency of snowfall occurrence decreases near 1 km and increases rapidly within the 0.5–1 km layer, demonstrating that strong-wind impacts on snowfall can be assessed using the MRR profiles.

4. Snowfall accumulation retrievals from the MRR are based on a locally fitted reflectivity–snowfall-rate relation, $Z_e = 166.64\,S^{1.76}$, enabling estimation of cumulative snowfall profiles for March 2024 to November 2025.

5. Relative to the MRR-based estimates, ERA5 shows a pronounced underestimation of cumulative snowfall; although the overall profile structure is broadly consistent with the MRR, ERA5 appears to overestimate low-level depletion associated with katabatic-flow-induced sublimation.

6. Consistent with the MRR-derived cumulative snowfall profiles, no pronounced katabatic influence is evident at Great Wall Station during the study period.

The observations presented for Great Wall Station indicate that the precipitation characteristics in this sector differ from those reported at several Antarctic sites where ground-based profiling has previously been conducted. As the first deployment of an MRR at Great Wall Station, this dataset expands current knowledge of regional contrasts in Antarctic precipitation and provides a valuable opportunity to evaluate climate-model and reanalysis products under polar environmental conditions. Nevertheless, quantifying precipitation over coastal Antarctica remains challenging and subject to substantial uncertainty. Given that the present analysis is limited to a two-year record, future work should extend the time series and pursue coordinated analyses that integrate longer-term MRR observations with remote sensing products and numerical model outputs to further constrain precipitation characteristics in the Great Wall Station region.

https://doi.org/10.5194/egusphere-2026-862
Preprint. Discussion started: 27 February 2026

Data availability

The MRR data can be made available upon request to corresponding authors. The surface observations in Great Wall Station can be accessed from https://datacenter.chinare.org.cn/data-center. The ERA5 data used are freely available through the C3S Climate Data Store (**https://cds.climate.copernicus.eu**) and ECMWF archive (**https://www.ecmwf.int/en/forecasts/datasets/archive-datasets**).

Author contributions

This research was designed by all authors. Jiayi Sun and Haoran Li carried out the data analysis. Jiayi Sun wrote the initial draft and all coauthors contributed to the writing.

Acknowledgments

The MRR data and AWS were collected by the observers at Zhongshan Station in Antarctica. We are grateful to them for providing the meteorological data and AWS information.

Financial support

This work was supported by National Natural Science Foundation of China (42525607, 42475095, 42305087), Basic Research Fund of CAMS (2023Z015, 2023Z004 and 2023Z025).

Competing interests

The authors also have no competing interests to declare.

References

Agosta, C., Fettweis, X., and Datta, R.: Evaluation of the CMIP5 models in the aim of regional modelling of the antarctic surface mass balance, The Cryosphere, 9, 2311–2321, https://doi.org/10.5194/tc-9-2311-2015, 2015.

https://doi.org/10.5194/egusphere-2026-862
Preprint. Discussion started: 27 February 2026

Alexander, S. P., Protat, A., Berne, A., and Ackermann, L.: Radar-derived snowfall microphysical properties at davis, antarctica, J. Geophys. Res. Atmospheres, 128, e2022JD038389, https://doi.org/10.1029/2022JD038389, 2023.

DeConto, R. M. and Pollard, D.: Contribution of antarctica to past and future sea-level rise, Nature, 531, 591–597, https://doi.org/10.1038/nature17145, 2016.

Ding, H., Li, H., and Liu, L.: Improved spectral processing for a multi-mode pulse compression Ka–Ku-band cloud radar system, Atmospheric Meas. Tech., 15, 6181–6200, https://doi.org/10.5194/amt-15-6181-2022, 2022a.

Ding, M., Han, W., Zhang, T., Yue, X., Fyke, J., Liu, G., and Xiao, C.: Towards more snow days in summer since 2001 at the great wall station, antarctic peninsula: The role of the amundsen sea low, Adv. Atmospheric Sci., 37, 494–504, https://doi.org/10.1007/s00376-019-9196-5, 2020.

Ding, M., Zou, X., Sun, Q., Yang, D., Zhang, W., Bian, L., Lu, C., Allison, I., Heil, P., and Xiao, C.: The PANDA automatic weather station network between the coast and dome a, east antarctica, Earth Syst. Sci. Data, 14, 5019–5035, https://doi.org/10.5194/essd-14-5019-2022, 2022b.

Grazioli, J., Madeleine, J.-B., Gallée, H., Forbes, R. M., Genthon, C., Krinner, G., and Berne, A.: Katabatic winds diminish precipitation contribution to the antarctic ice mass balance, Proc. Natl. Acad. Sci., 114, 10858–10863, https://doi.org/10.1073/pnas.1707633114, 2017a.

Grazioli, J., Genthon, C., Boudevillain, B., Duran-Alarcon, C., Del Guasta, M., Madeleine, J.-B., and Berne, A.: Measurements of precipitation in dumont d'urville, adélie land, east antarctica, The Cryosphere, 11, 1797–1811, https://doi.org/10.5194/tc-11-1797-2017, 2017b.

Li, H. and Moisseev, D.: Two layers of melting ice particles within a single radar bright band: Interpretation and implications, Geophys. Res. Lett., 47, e2020GL087499, https://doi.org/10.1029/2020GL087499, 2020.

Li, H., Tiira, J., Von Lerber, A., and Moisseev, D.: Towards the connection between snow microphysics and melting layer: Insights from multifrequency and dual-polarization radar observations during BAECC, Atmospheric Chem. Phys., 20, 9547–9562, https://doi.org/10.5194/acp-20-9547-2020, 2020.

https://doi.org/10.5194/egusphere-2026-862
Preprint. Discussion started: 27 February 2026

Loeb, N. A. and Kennedy, A.: Blowing snow at McMurdo station, antarctica during the AWARE field campaign: Multi-instrument observations of blowing snow, J. Geophys. Res. Atmospheres, 128, e2022JD037590, https://doi.org/10.1029/2022JD037590, 2023.

Maahn, M. and Kollias, P.: Improved micro rain radar snow measurements using doppler spectra post-processing, Atmospheric Meas. Tech., 5, 2661–2673, https://doi.org/10.5194/amt-5-2661-2012, 2012.

Morlighem, M., Rignot, E., Binder, T., Blankenship, D., Drews, R., Eagles, G., Eisen, O., Ferraccioli, F., Forsberg, R., Fretwell, P., Goel, V., Greenbaum, J. S., Gudmundsson, H., Guo, J., Helm, V., Hofstede, C., Howat, I., Humbert, A., Jokat, W., Karlsson, N. B., Lee, W. S., Matsuoka, K., Millan, R., Mouginot, J., Paden, J., Pattyn, F., Roberts, J., Rosier, S., Ruppel, A., Seroussi, H., Smith, E. C., Steinhage, D., Sun, B., Broeke, M. R. van den, Ommen, T. D. van, Wessem, M. van, and Young, D. A.: Deep glacial troughs and stabilizing ridges unveiled beneath the margins of the antarctic ice sheet, Nat. Geosci., 13, 132–137, https://doi.org/10.1038/s41561-019-0510-8, 2020.

Planat, N., Gehring, J., Vignon, É., and Berne, A.: Identification of snowfall microphysical processes from Eulerian vertical gradients of polarimetric radar variables, Atmospheric Meas. Tech., 14, 4543–4564, https://doi.org/10.5194/amt-14-4543-2021, 2021.

Roussel, M., Wiener, V., Genthon, C., Vignon, E., Bazile, E., Agosta, C., Berne, A., Durán-Alarcón, C., Dufresne, J., and Claud, C.: Assessing the simulation of snowfall at dumont d'urville, antarctica, during the YOPP-SH special observing campaign, Q. J. R. Meteorol. Soc., 149, 1391–1406, https://doi.org/10.1002/qj.4463, 2023.

Scarchilli, C., Ciardini, V., Grigioni, P., Iaccarino, A., Silvestri, L. D., Proposito, M., Dolci, S., Camporeale, G., Schioppo, R., Antonelli, A., Baldini, L., Roberto, N., Argentini, S., Bracci, A., and Frezzotti, M.: Characterization of snowfall estimated by in situ and ground-based remote-sensing observations at terra nova bay, victoria land, antarctica, J. Glaciol., 66, 1006–1023, https://doi.org/10.1017/jog.2020.70, 2020.

Schoger, S. Y., Moisseev, D., Lerber, A. von, Crewell, S., and Ebell, K.: Snowfall-rate retrieval for K- and W-band radar measurements designed in hyytiälä, finland, and tested at ny-ålesund, svalbard, norway, J. Appl. Meteorol. Climatol., https://doi.org/10.1175/JAMC-D-20-0095.1, 2021.

https://doi.org/10.5194/egusphere-2026-862
Preprint. Discussion started: 27 February 2026

Souverijns, N., Gossart, A., Lhermitte, S., Gorodetskaya, I. V., Kneifel, S., Maahn, M., Bliven, F. L., and van Lipzig, N. P. M.: Estimating radar reflectivity - snowfall rate relationships and their uncertainties over antarctica by combining disdrometer and radar observations, Atmospheric Res., 196, 211–223, https://doi.org/10.1016/j.atmosres.2017.06.001, 2017.

van Wessem, J. M., van de Berg, W. J., Noël, B. P. Y., van Meijgaard, E., Amory, C., Birnbaum, G., Jakobs, C. L., Krüger, K., Lenaerts, J. T. M., Lhermitte, S., Ligtenberg, S. R. M., Medley, B., Reijmer, C. H., van Tricht, K., Trusel, L. D., van Ulft, L. H., Wouters, B., Wuite, J., and van den Broeke, M. R.: Modelling the climate and surface mass balance of polar ice sheets using RACMO2 – part 2: Antarctica (1979–2016), The Cryosphere, 12, 1479–1498, https://doi.org/10.5194/tc-12-1479-2018, 2018.

Wiener, V., Roussel, M.-L., Genthon, C., Vignon, É., Grazioli, J., and Berne, A.: A 7-year record of vertical profiles of radar measurements and precipitation estimates at dumont d'urville, adélie land, east antarctica, Earth Syst. Sci. Data, 16, 821–836, https://doi.org/10.5194/essd-16-821-2024, 2024.